

# Fast erasure decoder for a class of quantum LDPC codes

Nicholas Connolly,<sup>1</sup> Vivien Londe,<sup>2</sup> Anthony Leverrier,<sup>1</sup> and Nicolas Delfosse<sup>3</sup>

<sup>1</sup>*Inria, Paris, France*

<sup>2</sup>*Microsoft, Paris, France*

<sup>3</sup>*Microsoft Quantum, Redmond, Washington 98052, USA*

(Dated: March 8, 2023)

We propose a decoder for the correction of erasures with hypergraph product codes, which form one of the most popular families of quantum LDPC codes. Our numerical simulations show that this decoder provides a close approximation of the maximum likelihood decoder that can be implemented in  $O(N^2)$  bit operations where  $N$  is the length of the quantum code. A probabilistic version of this decoder can be implemented in  $O(N^{1.5})$  bit operations.

*Introduction* – Due to the high noise rate of quantum hardware, extensive quantum error correction is necessary to scale quantum devices to the regime of practical applications. The surface code [1, 2] is one of the most popular quantum error correction code for quantum computing architectures but it comes with an enormous qubit overhead because each qubit must be encoded into hundreds or thousands of physical qubits.

Quantum Low-Density Parity-Check (LDPC) codes [3, 4] such as hypergraph product (HGP) codes [5] promise a significant reduction of this qubit overhead [6, 7]. Numerical simulations with circuit noise show a  $15\times$  reduction of the qubit count in the large-scale regime [8]. For applications to quantum fault tolerance, HGP codes must come with a *fast* decoder, whose role is to identify which error occurred. In this work, we propose a fast decoder for the correction of erasures or qubit loss. Our numerical simulations show that our decoder achieves a logical error rate close to the maximum likelihood decoder.

Our motivation for focusing on the decoding of erasures is twofold. First it is practically relevant and it is the dominant source of noise in some quantum platforms such as photonic systems [9, 10] for which a photon loss can be interpreted as an erasure, or neutral atoms [11]. Second, many of the ideas that led to the design of capacity-achieving classical LDPC codes over binary symmetric channels were first discovered by studying the correction of erasures [12, 13].

*Classical erasure decoders* – A linear code with length  $n$  is defined to be the kernel  $C = \ker H$  of an  $r \times n$  binary matrix  $H$  called the *parity-check matrix*. Our goal is to protect a *codeword*  $x \in C$  against erasures. We assume that each bit is erased independently with probability  $p$  and erased bits are flipped independently with probability  $1/2$ . The set of erased positions is known and is given by an *erasure vector*  $\varepsilon \in \mathbb{Z}_2^n$  such that bit  $b_i$  is erased iff  $\varepsilon_i = 1$ . The initial codeword  $x$  is mapped onto a vector  $y = x + e \in \mathbb{Z}_2^n$  where  $e$  is the indicator vector of the flipped bits of  $x$ . In particular the support of  $e$  satisfies  $\text{supp}(e) \subseteq \text{supp}(\varepsilon)$ . To detect  $e$ , we compute the *syndrome*  $s = Hy = He \in \mathbb{Z}_2^r$ . A non-trivial syndrome indicates the presence of bit-flips.

The goal of the decoder is to provide an estimation  $\hat{e}$  of  $e$  given  $s$  and  $\varepsilon$  and it succeeds if  $\hat{e} = e$ . This can be done by solving the linear system  $H\hat{e} = s$  with the condition  $\text{supp}(\hat{e}) \subseteq \text{supp}(\varepsilon)$  thanks to Gaussian elimination. This *Gaussian decoder* runs in  $O(n^3)$  bit operations which may be too slow in practice for large  $n$ .

---

## Algorithm 1: Classical peeling decoder

---

**input** : An erasure vector  $\varepsilon \in \mathbb{Z}_2^n$  and a syndrome  $s \in \mathbb{Z}_2^r$ .

**output**: Either **failure** or  $\hat{e} \in \mathbb{Z}_2^n$  such that  $H\hat{e} = s$  and  $\text{supp}(\hat{e}) \subseteq \text{supp}(\varepsilon)$ .

```
1 Set  $\hat{e} = 0$ .
2 while there exists a dangling check do
3   Select a dangling check  $c_i$ .
4   Let  $b_j$  be the dangling bit incident to  $c_i$ .
5   if  $s_i = 1$  then
6     Flip bit  $j$  of  $\hat{e}$ .
7     Flip  $s_k$  for all checks  $c_k$  incident with  $b_j$ .
8   Set  $\varepsilon_j = 0$ .
9 if  $\varepsilon \neq 0$  return Failure, else return  $\hat{e}$ .
```

---

The classical peeling decoder [14], described in Algorithm 1, provides a fast alternative to the Gaussian decoder. It does not perform as well in general, but it can be implemented in linear time and displays good performance for LDPC codes. To describe this decoder, it is convenient to introduce the *Tanner graph*, denoted  $T(H)$ , of the linear code  $C = \ker H$ . It is the bipartite graph with one vertex  $c_1, \dots, c_r$  for each row of  $H$  and one vertex  $b_1, \dots, b_n$  for each column of  $H$  such that  $c_i$  and  $b_j$  are connected iff  $H_{i,j} = 1$ . We refer to  $c_i$  as a *check node* and  $b_j$  as a *bit node*. The codewords of  $C$  are the bit strings such that the sum of the neighboring bits of a check node is  $0 \pmod 2$ . Given an erasure vector  $\varepsilon$ , a check node is said to be a *dangling check* if it is incident to a single erased bit. We refer to this erased bit as a *dangling bit*. The basic idea of the peeling decoder is to use dangling checks to recover the values of dangling bits and to repeat until the erasure is fully corrected.

The notion of stopping set was introduced in [15] to bound the failure probability of the decoder for classical

LDPC codes. A *stopping set* for the Tanner graph  $T(H)$  is defined to be a subset of bits that contains no dangling bit. If the erasure covers a non-empty stopping set, then Algorithm 1 returns **Failure**.

The peeling decoder was adapted to surface code [16] and color codes [17]. In the rest of this paper, we design a fast erasure decoder inspired by the peeling decoder that applies to a broad class of quantum LDPC codes. Our design process relies on the analysis of stopping sets. At each design iteration, we propose a new version of the decoder, identify its most common stopping sets and modify the decoder to make it capable of correcting these dominant stopping sets.

*Classical peeling decoder for quantum CSS codes* – A CSS code [18, 19] with length  $N$  is defined by commuting  $N$ -qubit Pauli operators  $S_{X,1}, \dots, S_{X,R_X} \in \{I, X\}^{\otimes N}$  and  $S_{Z,1}, \dots, S_{Z,R_Z} \in \{I, Z\}^{\otimes N}$  called the *stabilizer generators*. We refer to the group they generate as the *stabilizer group* and its elements are called *stabilizers*.

We can correct  $X$  and  $Z$  errors independently with the same strategy. Therefore we focus on the correction of  $X$  errors, based on the measurement of the  $Z$ -type stabilizer generators. This produces a *syndrome*  $\sigma(E) \in \mathbb{Z}_2^{R_Z}$ , whose  $i^{\text{th}}$  component is 1 iff the error  $E$  anti-commutes with  $S_{Z,i}$ . An error with trivial syndrome is called a *logical error* and a *non-trivial logical error* if it is not a stabilizer, up to a phase.

We assume that qubits are erased independently with probability  $p$  and that an erased qubit suffers from a uniform error  $I$  or  $X$  [20]. This results in an  $X$ -type error  $E$  such that  $\text{supp}(E) \subseteq \text{supp}(\varepsilon)$ . The decoder returns an estimate  $\hat{E}$  of  $E$  given the erasure vector  $\varepsilon$  and the syndrome  $s$  of  $E$ . It succeeds iff  $\hat{E}E$  is a stabilizer (up to a phase). The *logical error rate* of the scheme, denoted  $P_{\log}(p)$ , is the probability that  $\hat{E}E$  is a non-trivial logical error.

By mapping Pauli operators onto binary strings, one can cast the CSS erasure decoding problem as the decoding problem of a classical code with parity check matrix  $\mathbf{H}_Z$  whose rows correspond to the  $Z$ -type stabilizer generators. As a result, one can directly apply the classical Gaussian decoder and the classical peeling decoder to CSS codes. From Lemma 1 of [16], the Gaussian decoder is an optimal decoder, *i.e.* a Maximum Likelihood (ML) decoder, but its complexity scaling like  $O(N^3)$  makes it too slow for large codes. The peeling decoder is faster. However, the following lemma proves that, unlike its classical counterpart, it does not perform well for quantum LDPC codes.

**Lemma 1** (Stabilizer stopping sets). The support of an  $X$ -type stabilizer is a stopping set for the Tanner graph  $T(\mathbf{H}_Z)$ .

*Proof.* This is because an  $X$ -type stabilizer commutes with  $Z$ -type generators, and therefore its binary representation is a codeword for the classical linear code

$\ker \mathbf{H}_Z$ .  $\square$

As a consequence, the classical peeling decoder has no threshold for any family of quantum LDPC codes defined by bounded weight stabilizers. Indeed, if each member of the family has at least one  $X$ -type stabilizer with weight  $w$ , then the logical error rate satisfies  $P_{\log}(p) \geq p^w$ , which is a constant bounded away from zero when  $N \rightarrow \infty$ . This is in sharp contrast with the classical case for which the probability to encounter a stopping set provably vanishes for carefully designed families of LDPC codes [21].

*Pruned peeling decoder* – Since the peeling decoder gets stuck into stopping sets induced by the  $X$ -type generators, the idea is to look for such a generator  $S$  supported entirely within the erasure and to remove an arbitrary qubit of the support of  $S$  from the erasure. We can remove this qubit from the erasure because either the error  $E$  or its equivalent error  $ES$  (also supported inside  $\varepsilon$ ) acts trivially on this qubit.

---

**Algorithm 2:** Pruned peeling decoder

---

**input** : An erasure vector  $\varepsilon \in \mathbb{Z}_2^N$ , a syndrome  $s \in \mathbb{Z}_2^{R_Z}$ , and an integer  $M$ .

**output**: Either **Failure** or an  $X$ -type error  $\hat{E} \in \{I, X\}^N$  such that  $\sigma(\hat{E}) = s$  and  $\text{supp}(\hat{E}) \subseteq \text{supp}(\varepsilon)$ .

```

1 Set  $\hat{E} = I$ .
2 while there exists a dangling generator do
3   Select a dangling generator  $S_{Z,i}$ .
4   Let  $j$  be the dangling qubit incident to  $S_{Z,i}$ .
5   if  $s_i = 1$  then
6     Replace  $\hat{E}$  by  $\hat{E}X_j$  and  $s$  by  $s + \sigma(X_j)$ .
7   Set  $\varepsilon_j = 0$ .
8   if There is no dangling generator and there exists
     a product  $S$  of up to  $M$  stabilizer generators
      $S_{X,1}, \dots, S_{X,R_X}$  such that  $\text{supp}(S) \subseteq \text{supp}(\varepsilon)$  then
9     Select a qubit  $j \in \text{supp}(S)$  and set  $\varepsilon_j = 0$ .
10 if  $\varepsilon \neq 0$  return Failure, else return  $\hat{E}$ .
```

---

This leads to the pruned peeling decoder described in Algorithm 2. To make it easier to follow, we use the terms *dangling generator* and *dangling qubit* in place of dangling check and dangling bit. A dangling generator is a  $Z$  generator in the context of correcting  $X$  errors. In order to keep the complexity of the peeling decoder linear, we look for an  $X$ -type stabilizer which is a product of up to  $M$  stabilizer generators where  $M$  is a small constant. For low erasure rate, we expect the erased stabilizers to have small weight and therefore a small value of  $M$  should be sufficient.

Fig. 1 shows the performance of HGP codes equipped with the pruned peeling decoder with  $M = 0, 1, 2$ . The pruning strategy only slightly improves over the classical peeling decoder and increasing  $M$  beyond  $M = 1$  does not significantly affect the performance. To understand why the ML decoder severely outperforms the pruned

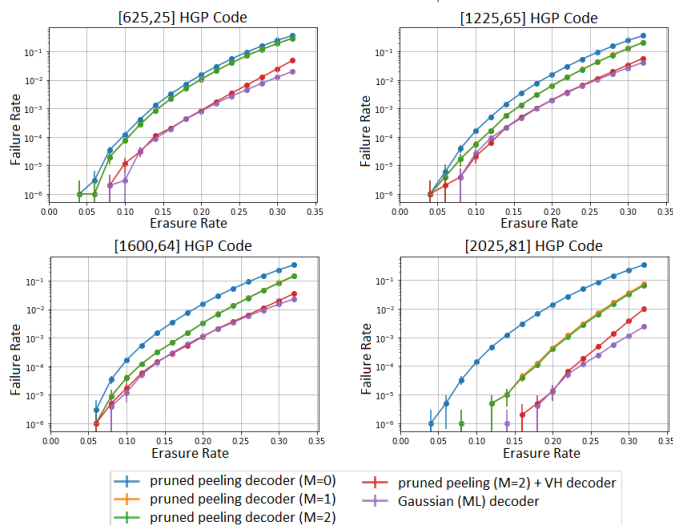


Figure 1. Performance of the pruned peeling and VH decoders using four HGP codes and compared with the ML decoder ( $10^6$  simulations per data point). Plots show the failure rates of the decoders for recovering an X-type Pauli error supported on the erasure vector, up to multiplication by a stabilizer.

peeling decoder, we analyze its most common stopping sets with HGP codes.

*Stopping sets of the pruned peeling decoder* – Let us recall the hypergraph product construction from [5]. The HGP code associated with the Tanner graph  $T(H) = (A \cup B, E_H)$  of a classical code is a CSS code, denoted  $\text{HGP}(H)$ , defined from the cartesian product of  $T(H)$  with itself (see Fig. 2). Qubits are labelled by the pairs  $(a, a') \in A \times A$  and  $(b, b') \in B \times B$ . For each  $(a, b') \in A \times B$ , we define a stabilizer generator acting as  $X$  on the qubits  $(b, b')$  such that  $\{a, b\} \in E_H$  and the qubits  $(a, a')$  such that  $\{a', b'\} \in E_H$ . For each  $(b, a') \in B \times A$ , we define a stabilizer generator acting as  $Z$  on the qubits  $(a, a')$  such that  $\{a, b\} \in E_H$  and the qubits  $(b, b')$  such that  $\{a', b'\} \in E_H$ . If the input graph  $T(H)$  is sparse, then  $\text{HGP}(H)$  is LDPC.

The input Tanner graph is generated using the standard progressive edge growth algorithm which is commonly used to produce good classical or quantum LDPC codes [22]. We use the implementation [23, 24] of the progressive edge growth algorithm.

By studying the failure configurations of the pruned peeling decoder, we observe that the gap between the pruned peeling decoder and the ML decoder is due to the following stopping sets of HGP codes.

**Lemma 2** (Horizontal and vertical stopping sets). If  $S_B$  is a stopping set for a Tanner graph  $T(H)$ , then for all  $b \in B$  the set  $\{b\} \times S_B$  is a stopping set for the Tanner graph  $T(\mathbf{H}_Z)$  of the HGP code  $\text{HGP}(H)$ . If  $S_A$  is a stopping set for a Tanner graph  $T(H^T)$ , then for all  $a' \in A$  the set  $S_A \times \{a'\}$  is a stopping set for the Tanner graph  $T(\mathbf{H}_Z)$

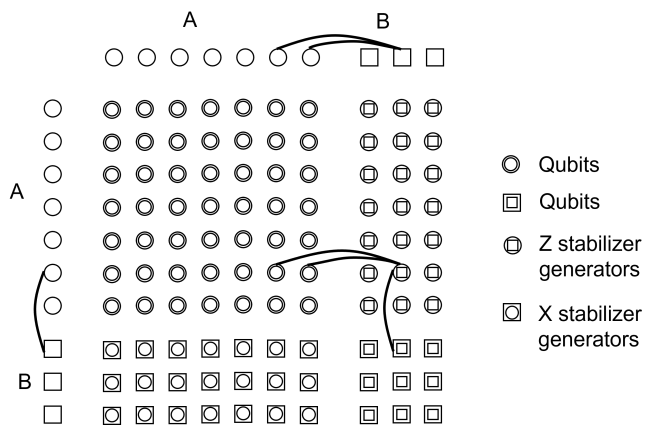


Figure 2. The HGP code derived from a linear code with 7 bits and 3 checks. The support of the  $Z$  stabilizer generator with index  $(b, a') \in B \times A$  is given by the neighbors of  $(b, a')$  in the Cartesian product of the graph  $T(H)$  with itself. In the product notation, we follow the  $x \times y$  convention, where the first coordinate denotes the horizontal code and the second coordinate denotes the vertical code.

of the HGP code  $\text{HGP}(H)$ .

*Proof.* Consider a stopping set  $S_B$  for  $T(H)$ . Any  $Z$ -type stabilizer generator acting on  $\{b\} \times S_B$  must be indexed by  $(b, a')$  for some  $a'$ . Moreover, the restriction of these stabilizers to  $\{b\} \times S_B$  are checks for the linear code  $\ker H$ . Therefore  $\{b\} \times S_B$  is a stopping set for  $T(\mathbf{H}_Z)$ . The second case is similar.  $\square$

We refer to the stopping sets  $\{b\} \times S_B$  as *vertical stopping sets* and  $S_A \times \{a'\}$  as *horizontal stopping sets*. Numerically, we observe that these stopping sets are responsible for vast majority of the failures of the pruned peeling decoder. This is because the quantum Tanner graph  $T(\mathbf{H}_Z)$  contains on the order of  $\sqrt{N}$  copies of the type  $\{b\} \times S_B$  for each stopping sets  $S_B$  of  $T(H)$  and  $\sqrt{N}$  copies of each stopping set of  $T(H^T)$ . Our idea is to use the Gaussian decoders of the classical codes  $\ker H$  and  $\ker H^T$  to correct these stopping sets.

*VH decoder* – The Vertical-Horizontal (VH) decoder is based on the decomposition of the erasure into vertical subsets of the form  $\{b\} \times \varepsilon_b$  with  $b \in B$  and  $\varepsilon_b \subseteq B$ , and horizontal subsets of the form  $\varepsilon_{a'} \times \{a'\}$  with  $a' \in A$  and  $\varepsilon_{a'} \subseteq A$ , that will be decoded using the Gaussian decoder.

Let  $T_v$  (resp.  $T_h$ ) be the subgraph of  $T(\mathbf{H}_Z)$  induced by the vertices of  $B \times (A \cup B)$  (resp.  $(A \cup B) \times A$ ). The graph  $T_v$  is made with the vertical edges of  $T(\mathbf{H}_Z)$  and  $T_h$  is made with its horizontal edges. Given an erasure vector  $\varepsilon$ , denote by  $V(\varepsilon)$  the set of vertices of  $T(\mathbf{H}_Z)$  that are either erased qubits or check nodes incident to an erased qubit. A *vertical cluster* (resp. *horizontal cluster*) is a subset of  $V(\varepsilon)$  that is a connected component for the graph  $T_v$  (resp.  $T_h$ ).

The *VH graph* of  $\varepsilon$  is defined to be the graph whose vertices are the clusters and two clusters are connected iff their intersection is non-empty.

The following proposition provides some insights on the structure of the VH graph.

**Proposition 1.** The VH graph is a bipartite graph where each edge connects a vertical cluster with an horizontal cluster. There is a one-to-one correspondence between the check nodes of  $T(\mathbf{H}_Z)$  that belong to one vertical cluster and one horizontal cluster and the edges of the VH graph.

*Proof.* Because the graph  $T_v$  contains only vertical edges, any vertical cluster must be a subset of  $\{b_1\} \times (A \cup B)$  for some  $b_1 \in B$ . Similarly, any horizontal cluster is a subset of  $(A \cup B) \times \{a'_1\}$  for some  $a'_1 \in A$ . As a result, two clusters with the same orientation (horizontal or vertical) cannot intersect and the only possible intersection between a cluster included in  $\{b_1\} \times (A \cup B)$  and a cluster included in  $(A \cup B) \times \{a'_1\}$  is the check node  $(b_1, a'_1)$ . The bijection between check nodes and edges of the VH graph follows.  $\square$

A check node of  $T(\mathbf{H}_Z)$  that belongs to a single cluster is called an *internal check*, otherwise it is called a *connecting check*. From Proposition 1, a connecting check must belong to one horizontal and one vertical cluster.

Given a cluster  $\kappa$ , let  $E(\kappa)$  be the set of errors supported on the qubits of  $\kappa$  whose syndrome is trivial over the internal checks of  $\kappa$ . Let  $S(\kappa)$  be the set of syndromes of errors  $E \in E(\kappa)$  restricted to the connecting checks of  $\kappa$ . A cluster is said to be *isolated* if it has no connecting check. Then, it can be corrected independently of the other clusters. A *dangling cluster* is defined to be a cluster with a single connecting check.

A cluster  $\kappa$  can have two types of connecting check. If  $S(\kappa)$  contains a weight-one vector supported on an connecting check  $c$ , we say that  $c$  is a *free check*. Otherwise, it is a *frozen check*. If a check is free, the value of the syndrome on this check can be adjusted at the end of the procedure to match  $s$  using an error included in the cluster  $\kappa$ .

To compute a correction  $\hat{E}$  for a syndrome  $s \in \mathbb{Z}_2^{R_Z}$ , we proceed as follows. Denote by  $s_\kappa$  the restriction of  $s$  to a cluster  $\kappa$ . We initialize  $\hat{E} = I$  and we consider three cases.

**Case 1: Isolated cluster.** If  $\kappa$  is a isolated cluster, we use Gaussian elimination to find an error  $\hat{E}_\kappa$  supported on the qubits of  $\kappa$  whose syndrome matches  $s$  on the internal checks of  $\kappa$ . Then, we add  $\hat{E}_\kappa$  to  $\hat{E}$ , we add  $\sigma(\hat{E}_\kappa)$  to  $s$  and we remove  $\kappa$  from the erasure  $\varepsilon$ . This cluster can be corrected independently of the other cluster because it is not connected to any other cluster.

**Case 2: Frozen dangling cluster.** If  $\kappa$  is a dangling cluster and its only connecting check is frozen, we proceed exactly as in the case of an isolated cluster. This is

possible because any correction has the same contribution to the syndrome on the connecting check.

**Case 3: Free dangling cluster.** The correction of a dangling cluster  $\kappa$  that contains a free check is delayed until the end of the procedure. We remove  $\kappa$  from the erasure and we remove its free check from the Tanner graph  $T(\mathbf{H}_Z)$ . Then, we look for a correction  $\hat{E}'$  in the remaining erasure. We add  $\hat{E}'$  to  $\hat{E}$  and  $\sigma(\hat{E}')$  to  $s$ . Once the remaining erasure is corrected and the syndrome is updated, we find a correction  $\hat{E}_\kappa$  inside  $\kappa$  that satisfies the remaining syndrome  $s_\kappa$  in  $\kappa$ . We proceed in that order because the value of the syndrome on a free check can be adjusted at the end of the procedure to match  $s$  using an error included in the cluster  $\kappa$  (by definition of free checks).

Altogether, we obtain the VH decoder (Algorithm 3). Our implementation is available here [25]. It works by correcting all isolated and dangling clusters until the erasure is fully corrected. Otherwise, it returns **Failure**.

---

### Algorithm 3: VH decoder

---

**input** : An erasure vector  $\varepsilon \in \mathbb{Z}_2^N$ , a syndrome  $s \in \mathbb{Z}_2^{R_Z}$ .

**output**: Either **Failure** or an  $X$ -type error  $\hat{E} \in \{I, X\}^N$  such that  $\sigma(\hat{E}) = s$  and  $\text{supp}(\hat{E}) \subseteq \text{supp}(\varepsilon)$ .

- 1 Set  $\hat{E} = I$ .
- 2 Construct an empty stack  $L = []$ .
- 3 **while** there exists an isolated or a dangling cluster  $\kappa$  **do**
- 4     **if**  $\kappa$  is isolated or frozen **then**
- 5         Compute an error  $\hat{E}_\kappa$  supported on  $\kappa$  whose syndrome matches  $s$  on the internal checks of  $\kappa$  in  $T(\mathbf{H}_Z)$ .
- 6         Replace  $\hat{E}$  by  $\hat{E}\hat{E}_\kappa$  and  $s$  by  $s + \sigma(\hat{E}_\kappa)$ .
- 7         **For** all qubits  $j$  in  $\kappa$ , set  $\varepsilon_j = 0$ .
- 8     **else**
- 9         Then  $\kappa$  is free.
- 10         Remove the free connecting check  $c$  of  $\kappa$  from the Tanner graph  $T(\mathbf{H}_Z)$ .
- 11         Add the pair  $(\kappa, c)$  to the stack  $L$ .
- 12         **For** all qubits  $j$  in  $\kappa$ , set  $\varepsilon_j = 0$ .
- 13 **while** the stack  $L$  is non-empty **do**
- 14     Pop a cluster  $(\kappa, c)$  from the stack  $L$ .
- 15     Add the check node  $c$  to the Tanner graph  $T(\mathbf{H}_Z)$ .
- 16     Compute an error  $\hat{E}_\kappa$  supported on  $\kappa$  whose syndrome matches  $s$  on all the checks of  $\kappa$  in  $T(\mathbf{H}_Z)$ , including the free check  $c$ .
- 17     Replace  $\hat{E}$  by  $\hat{E}\hat{E}_\kappa$  and  $s$  by  $s + \sigma(\hat{E}_\kappa)$ .
- 18 **if**  $\varepsilon \neq 0$  **return Failure**, **else return**  $\hat{E}$ .

---

For a  $r \times n$  matrix  $H$ , the complexity of the VH decoder is dominated by the cost of the Gaussian decoder which grows as  $O(n^3)$  per cluster and  $O(n^4)$  including all the clusters (assuming  $r = O(n)$ ). Therefore the VH decoder can be implemented in  $O(N^2)$  bit operations where

$N = \Theta(n^2)$  is the length of the quantum HGP code. Using a probabilistic implementation of the Gaussian decoder [26–29], we can implement the Gaussian decoder in  $O(n^2)$  operations, reducing the complexity of the VH decoder to  $O(N^{1.5})$ .

Algorithm 3 fails if the VH-graph of the erasure contains a cycle. However, one can modify the algorithm to eliminate some cycles by removing free checks of all clusters and not only dangling clusters. This may improve further the performance of the VH-decoder.

In comparison with our numerical results from Fig. 1, we see that the combination of pruned peeling and VH decoders performs almost as well as the ML decoder at low erasure erasure rates. This is to say that cycles of clusters, which are stopping sets for the VH decoder, are relatively infrequent in the low erasure rate regime. This behavior matches our intuition since errors for LDPC codes tend to be composed of disjoint small weight clusters [30].

*Conclusion* – We proposed a practical high-performance decoder for the correction of erasure with HGP codes. Our numerical simulations show that the combination of the pruned peeling decoder with the VH decoder achieves a close-to-optimal performance in complexity  $O(N^2)$ . This decoder can be used as a subroutine of the Union-Find decoder for LDPC codes [31] to speed up this algorithm.

In future work, it would be interesting to adapt our decoder to other quantum LDPC codes [32–35]. We are also wondering if one can reduce the complexity further to obtain a linear time ML decoder for the correction of erasure.

Finally, it would be interesting to investigate the resource overhead of quantum computing architectures capable of detecting erasures based on neutral atoms [11], trapped ions [36] or superconducting qubits [37].

This research was supported by the MSR-Inria Joint Centre. AL acknowledges support from the Plan France 2030 through the project ANR-22-PETQ-0006.

- 
- [1] E. Dennis, A. Kitaev, A. Landahl, and J. Preskill, *Journal of Mathematical Physics* **43**, 4452 (2002).
- [2] A. G. Fowler, M. Mariantoni, J. M. Martinis, and A. N. Cleland, *Physical Review A* **86**, 032324 (2012).
- [3] R. Gallager, *IRE Transactions on Information Theory* **8**, 21 (1962).
- [4] D. J. MacKay, G. Mitchison, and P. L. McFadden, *IEEE Transactions on Information Theory* **50**, 2315 (2004).
- [5] J.-P. Tillich and G. Zémor, *IEEE Transactions on Information Theory* **60**, 1193 (2013).
- [6] D. Gottesman, *Quantum Information & Computation* **14**, 1338 (2014).
- [7] O. Fawzi, A. Grospellier, and A. Leverrier, in *2018 IEEE 59th Annual Symposium on Foundations of Computer Science (FOCS)* (IEEE, 2018) pp. 743–754.
- [8] M. A. Tremblay, N. Delfosse, and M. E. Beverland, arXiv preprint arXiv:2109.14609 (2021).
- [9] E. Knill, R. Laflamme, and G. J. Milburn, *nature* **409**, 46 (2001).
- [10] S. Bartolucci, P. Birchall, H. Bombin, H. Cable, C. Dawson, M. Gimeno-Segovia, E. Johnston, K. Kieling, N. Nickerson, M. Pant, *et al.*, arXiv preprint arXiv:2101.09310 (2021).
- [11] Y. Wu, S. Kolkowitz, S. Puri, and J. D. Thompson, arXiv preprint arXiv:2201.03540 (2022).
- [12] S. Kudekar, T. Richardson, and R. L. Urbanke, *IEEE Transactions on Information Theory* **59**, 7761 (2013).
- [13] T. Richardson and R. Urbanke, *Modern coding theory* (Cambridge university press, 2008).
- [14] M. G. Luby, M. Mitzenmacher, M. A. Shokrollahi, and D. A. Spielman, *IEEE Transactions on Information Theory* **47**, 569 (2001).
- [15] V. V. Zyablov and M. S. Pinsker, *Problemy Peredachi Informatsii* **10**, 15 (1974).
- [16] N. Delfosse and G. Zémor, *Physical Review Research* **2**, 033042 (2020).
- [17] S. Lee, M. Mhalla, and V. Savin, in *2020 IEEE International Symposium on Information Theory (ISIT)* (IEEE, 2020) pp. 1886–1890.
- [18] A. Steane, *Proceedings of the Royal Society of London. Series A: Mathematical, Physical and Engineering Sciences* **452**, 2551 (1996).
- [19] A. R. Calderbank and P. W. Shor, *Physical Review A* **54**, 1098 (1996).
- [20] M. Grassl, T. Beth, and T. Pellizzari, *Physical Review A* **56**, 33 (1997).
- [21] T. J. Richardson and R. L. Urbanke, *IEEE Transactions on Information Theory* **47**, 638 (2001).
- [22] X.-Y. Hu, E. Eleftheriou, and D.-M. Arnold, in *GLOBECOM'01. IEEE Global Telecommunications Conference (Cat. No. 01CH37270)*, Vol. 2 (2001) pp. 995–1001 vol.2.
- [23] X.-Y. Hu, E. Eleftheriou, and D. Arnold, *IEEE Transactions on Information Theory* **51**, 386 (2005).
- [24] T. S. Manu, *Progressive edge growth algorithm for generating LDPC matrices* (2014).
- [25] N. Connolly, *Pruned peeling and vh decoder* (2022).
- [26] D. Wiedemann, *IEEE Transactions on Information Theory* **32**, 54 (1986).
- [27] E. Kalfoten and B. David Saunders, in *International Symposium on Applied Algebra, Algebraic Algorithms, and Error-Correcting Codes* (Springer, 1991) pp. 29–38.
- [28] B. A. LaMacchia and A. M. Odlyzko, in *Conference on the Theory and Application of Cryptography* (Springer, 1990) pp. 109–133.
- [29] E. Kalfoten, *Mathematics of Computation* **64**, 777 (1995).
- [30] A. A. Kovalev and L. P. Pryadko, *Physical Review A* **87**, 020304 (2013).
- [31] N. Delfosse, V. Londe, and M. E. Beverland, *IEEE Transactions on Information Theory* (2022).
- [32] N. P. Breuckmann and J. N. Eberhardt, *IEEE Transactions on Information Theory* **67**, 6653 (2021).
- [33] P. Panteleev and G. Kalachev, in *Proceedings of the 54th Annual ACM SIGACT Symposium on Theory of Computing* (2022) pp. 375–388.
- [34] A. Leverrier and G. Zémor, arXiv preprint arXiv:2202.13641 (2022).
- [35] I. Dinur, M.-H. Hsieh, T.-C. Lin, and T. Vidick, arXiv preprint arXiv:2206.07750 (2022).

- [36] M. Kang, W. C. Campbell, and K. R. Brown, arXiv preprint arXiv:2210.15024 (2022).
- [37] A. Kubica, A. Haim, Y. Vaknin, F. Brandão, and A. Retzker, arXiv preprint arXiv:2208.05461 (2022).